Mössbauer Absorption in Fe⁵⁷ in Metallic Iron from the Curie Point to the γ-δ Transition*

T. A. Kovats and J. C. Walker†

The Johns Hopkins University, Baltimore, Maryland 21218

(Received 11 October 1968)

Mössbauer absorption in Fe⁵⁷ in metallic iron has been observed for absorber temperatures from 22 to 1413°C, with particular emphasis on the region from the Curie point through the γ-δ phase transition. Values of recoilless fraction f_A and Debye temperature Θ for iron were determined as a function of temperature from Mössbauer absorption line areas. The recoilless fraction takes on values from 0.84 ± 0.04 at room temperature to 0.012 ± 0.006 at a point just above the γ-δ transition temperature $T_{\gamma\delta}$. At the α-γ and γ-δ phase transition points there are discontinuities in f_A of $\delta f_A = +0.030\pm0.008$ and -0.06 ± 0.01, respectively. The values of Θ behave correspondingly, decreasing from (510 ± 80)°K at room temperature to (226 ± 14)°K at the point just above $T_{\gamma\delta}$, with $\delta\Theta = (8\pm3)$°K at $T_{\alpha\gamma}$ and $-(70\pm15)$°K at $T_{\gamma\delta}$. The determinations of f_A and Θ in the region from the Curie point up to the γ-δ transition were the most accurate, with statistical errors of about ±0.004 in f_A and ±2°K in Θ. The energy shift in the iron absorber was determined as a function of temperature from the centroid of the Mössbauer absorption spectrum. At the α-γ transition, a discontinuity occurs in the energy shift of $-(0.041\pm0.004)$ mm/sec, three times too large to be explained solely by an isomer shift discontinuity due to an assumed scaling of the 4s atomic electron density with the volume. At the γ-δ transition, a discontinuity in the energy shift of $-(0.10\pm0.02)$ mm/sec is observed, too large and in the wrong direction to be accounted for by scaling the 4s density with volume. The discrepancies in the shift discontinuities are of the same sign at $T_{\alpha\gamma}$ and $T_{\gamma\delta}$, and indicate the existence of a mechanism for increasing the electron density at the nucleus at both phase transitions on going into the higher-temperature phase.

I. INTRODUCTION

IN the present experiment, measurements of the intensity and the energy shift of Mössbauer absorption in Fe⁵⁷ in metallic iron have been made from room temperature through the γ-δ phase transition at about 1400°C, with primary emphasis on the region above the Curie point. The work is, to some extent, an extension of the work of Preston and co-workers,[1] who studied the region up to the Curie point carefully and obtained some data at temperatures as high as 900°C. In the present case values of the absorption recoilless fraction f_A and Debye temperatures Θ were determined from room temperature to the γ-δ phase transition. The total energy shift (at constant pressure) was measured from room temperature to the γ-δ phase transition. At the α-γ and γ-δ transitions, discontinuities in the total energy shift occur owing to sudden changes in the atomic electron density at the nucleus.

It is convenient to measure the strength of recoilless absorption by means of the area in the spectral Mössbauer absorption line. It can be shown[2,3] that the absolute area A in an observed single-line absorption dip is given by

$$A = \pi SB f_S \gamma_A L(t_A), \qquad (1)$$

where B is the base line (uncorrected off-resonance count rate), S is the signal fraction in the actual spectrum emitted by the source (so that SB is the background corrected off-resonance count rate), f_S is the source recoilless fraction, $\gamma_A = \frac{1}{2}\Gamma_A$ is the half-width half-maximum of the Mössbauer (14.4-keV) level in the absorber nucleus, and t_A is the number of resonant absorption lengths in the absorber, given by

$$t_A = f_A n_A \sigma_0, \qquad (2)$$

where f_A is the absorber recoilless fraction, n_A is the number of nuclei per unit area capable of resonant absorption in the absorber, and σ_0 is the peak value of the resonance absorption cross section. Bykov and Hien point out[3] that the nonlinear function $L(t_A)$ can be expressed in closed form, so that Eq. (1) becomes

$$A = \pi SB f_S \gamma_A t_A e^{-t_A/2}[I_0(\tfrac{1}{2}t_A) + I_1(\tfrac{1}{2}t_A)], \qquad (3)$$

where I_0 and I_1 are the usual Bessel functions of imaginary argument and are tabulated by Watson.[4] In this experiment all quantities in Eqs. (2) and (3) are known or experimentally measured except for the recoilless fraction f_A, and so the latter quantity may be determined from Eq. (3). The recoilless fraction may be related to the Debye temperature by[5]

$$f_A = \exp\left\{-\frac{E_A^2}{2m_A c^2}\frac{6}{k\Theta}\left[\frac{1}{4} + \left(\frac{T}{\Theta}\right)^2 \int_0^{\Theta/T}\frac{x\,dx}{e^x-1}\right]\right\}, \qquad (4)$$

where E_A is the resonant absorption energy in the absorber nucleus, m_A is the mass of the absorber nucleus, and c and k denote the usual atomic constants. Tables of

[1] R. S. Preston, S. S. Hanna, and J. Heberle, Phys. Rev. **128**, 2207 (1962).

[2] G. Lang, Nucl. Instr. Methods **24**, 425 (1963).

[3] G. A. Bykov and Pham Zuy Hien, Zh. Eksperim. i Teor. Fiz. **43**, 909 (1962) [English transl.: Soviet Phys.—JETP **16**, 646 (1963)].

[4] G. N. Watson, *Theory of Bessel Functions* (Cambridge University Press, Cambridge, 1952), pp. 698–713.

[5] K. S. Singwi and A. Sjölander, Phys. Rev. **120**, 1093 (1960).

the integral in Eq. (4) are given by Holm.[6] Once f_A has been found from Eq. (3), Θ may be obtained from Eq. (4). Since the concept of Debye temperature implies that Θ is *not* a function of temperature, the measurement of Θ versus temperature implies that this model is not perfect for iron.

II. EXPERIMENTAL PROCEDURE

A. Source and Absorber

The source used in this experiment was prepared by the New England Nuclear Corporation and consisted of 20 mCi of Co^{57} diffused into a 0.0005-in. Pd disk; the active area was a circle 0.25 in. in diam and the diffusion process was carried out only long enough to obtain a minimal-source linewidth. [As determined by the seller, the source yields a 0.23-mm/sec full width at half-maximum (FWHM) spectral line with a thin sodium ferrocyanide absorber.] During the data runs in this experiment, the source was held at room temperature, $(22\pm1)°C$. The value of the source recoilless fraction f_S ($=0.652$) is given by Steyert and Taylor.[7]

The absorber was cut from 0.0005-in. sheets of 99.9%-pure natural iron supplied by A. D. Mackay, Inc. The mass per unit area was directly measured here to be 9.6 ± 0.4 mg/cm². The absorber temperature was varied from 22 to 1413°C by the oven described in Sec. II D.

B. Detection and Counting Electronics

A Reuter-Stokes RSG-30A 1-atm xenon-methane proportional counter was used to detect the 14.4-keV radiation transmitted through the absorber in the oven. The data were collected in a Nuclear Data ND-110 128-channel analyzer operating in the multiscale mode,

which was synchronized by a pulse from the triangle generator used to drive the source Doppler-shifting system.

A full pulse-height spectrum recorded in this analyzer running in the pulse-height mode was fitted with Gaussians for signal and noise peaks and a horizontal base line for Compton background, so that the fraction of counts in each channel which are signal (14.4 keV) was known. With this information it was possible to calculate the total signal fraction S in the window used (i.e., in the pulse-height spectrum, with the upper and lower discriminators on the single-channel analyzer closed down around the 14.4-keV peak). If the total off-resonant count rate is denoted by B, as above, then the off-resonant count rate corrected for background is SB. The signal fraction was determined to be $S=0.70\pm0.07$ for all the Mössbauer runs. A pulse-height spectrum with the window set was run for a fixed live time before every run; the resulting pulse-height spectra agreed within the (1%) statistics, indicating no drift in the electronics.

C. Source Doppler Velocity Drive

The source was moved with constant acceleration. The circuit[8] used to control the source motion was a modified version of that of Cohen *et al.*,[9] and the triangle generator which provided the source velocity waveform is similar to one proposed by Cohen[10] except that the triangle was asymmetrized to provide rapid flyback. The feedback velocity-sensing LVsyn coil in the source drive circuit was rigidly clamped to the combustion tube containing the absorber, as shown in Fig. 1. The system was calibrated from room-temperature metallic iron Mössbauer spectra with the data of Preston *et al.*[1]
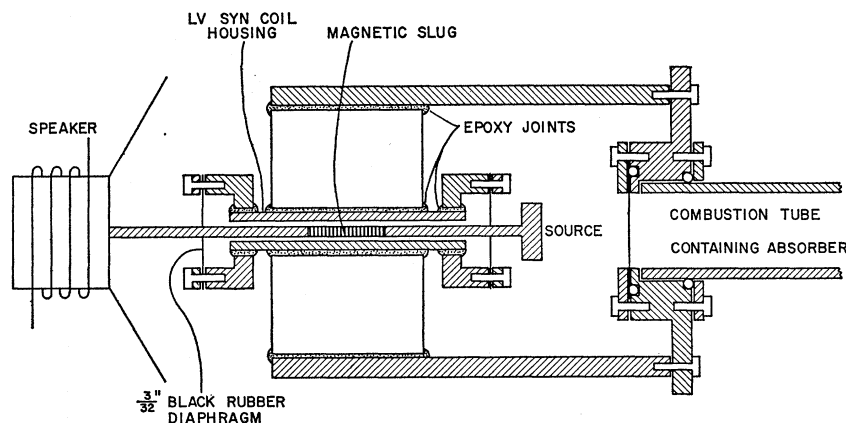

FIG. 1. LV syn coil mount.

[6] M. W. Holm, *Debye Characteristic Temperature Table and Bibliography* (Office of Technical Services, U. S. Department of Commerce, Washington, D. C., 1957), pp. 8 and 9.
[7] W. A. Steyert and R. D. Taylor, Phys. Rev. **134A**, 716 (1964).
[8] T. A. Kovats, Ph.D. thesis, Johns Hopkins University, 1968 (unpublished).
[9] R. L. Cohen, P. G. McMillin, and G. K. Wertheim, Rev. Sci. Instr. **34**, 671 (1963).
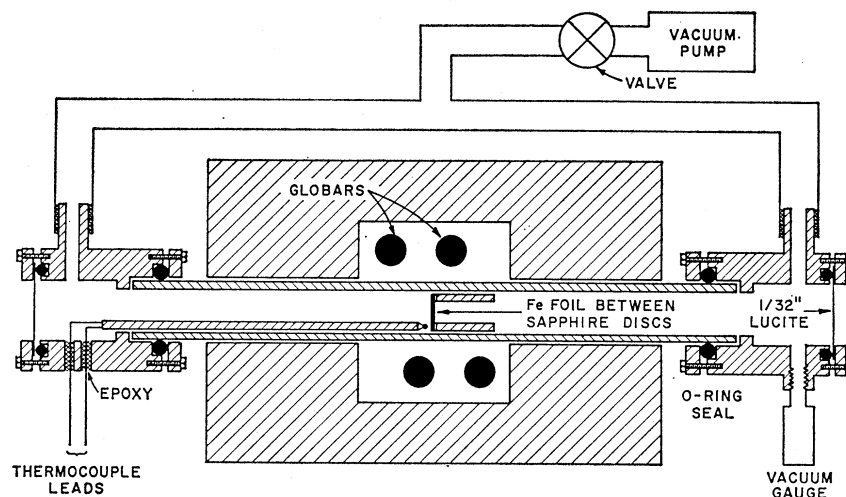[10] R. L. Cohen, Rev. Sci. Instr. **37**, 260 (1966).

FIG. 2. Oven used to heat the
iron absorber.

D. Absorber-Heating Apparatus

A schematic diagram of the apparatus used to heat the Fe absorber foil is shown in Fig. 2. The oven is a Leco 540-300, heated by four SiC rods connected in series to a tapped high-current autotransformer powered by a 208-V ac line. It has a 5-in. heating length and can run up to 1600°C.

The combustion tube containing the absorber is a 30-in.-long mullite ($3Al_2O_3 \cdot 2SiO_2$) tube, with an inner diameter of $1\frac{1}{4}$ in. and an $\frac{1}{8}$-in. wall. Cast mullite has a porosity low enough to be vacuum-tight to 10^{-5} Torr, even at high temperatures, allowing the tube containing the absorber to be maintained under vacuum during the runs of the present experiment. The machined brass ends on the combustion tube shown in Fig. 2 provide leak-tight connections between the combustion tube and the vacuum pump, which is an oil-diffusion pump backed up by a standard mechanical rotary roughing pump. The vacuum connections, shown only schematically in the figure, consist primarily of lengths of flexible brass tubing with screw-on O-ring connections at both ends. The remaining connecting pieces are made of soft soldered brass pipe. The combustion tube was pumped on all the time during the high-temperature runs, and a pressure below 10^{-4} Torr was maintained.

To prevent evaporation and chemical deterioration ta high temperatures, the iron absorber foil was sandwiched between two 0.005-in. sapphire disks obtained from Adolf Meller, Inc. This sandwich was cemented to a $1\frac{1}{8}$-in.-o.d., $\frac{1}{8}$-in.-wall, 2-in.-long mullite tube, with Aremco 505 alumina cement. To prevent trapping oxygen, this mounting procedure was carried out in a helium atmosphere. The sapphire disks successfully prevented evaporation and oxidation until they cracked above 1336°C, the cracking being evidenced by a gradual increase in count rate due to evaporation of the iron.

Although only one thermocouple is visible in Fig. 2, two are inside the combustion tube, side by side on the

bottom. One, Mo-W–25% Re, is used in the feedback circuit which controls the oven temperature, and the other, Chromel-P-Alumel, is monitored for absolute temperature readings. Feedthrough of the thermocouple leads from the outside into the vacuum chamber was accomplished as shown in Fig. 2, through holes drilled in the brass ends on the combustion tube, which are filled with Epoxy.

A feedback circuit[8] was used to control the absorber temperature to within about ±2°C.

E. Data Analysis

A least-squares fitting program was used to fit the multiline spectra obtained below the Curie point with six Lorentzian lines constrained to satisfy the symmetry and splitting ratio characteristic of a metallic iron Mössbauer spectrum. Above the Curie point, the single spectral line was fitted with one Lorentzian. The value of χ^2 obtained for the fits to the multiline spectra was two to three times the expected value. The number of channels per peak was significantly greater for the single-line spectra because these were taken at a higher peak-to-peak source Doppler velocity, and the χ^2 obtained for these range from 0.9 to 2 times the expected value, with most being quite near the expected value.

Because the object of this experiment was to determine the temperature dependence of the recoilless fraction and the energy shift, the errors assigned to the results are the statistical errors obtained from the error matrix in the fitting program and do not include the possible absolute errors in the signal fraction S (10%) and in the measured mass per unit area in the absorber (4%).

Values of the constants pertaining to the Mössbauer transition from the 14.4-keV level of Fe^{57} were taken from the *Mössbauer Effect Data Index*.[11]

――――――
[11] A. H. Muir, K. J. Ando, and H. M. Coogan, *Mössbauer Effect Data Index, 1958–1965* (Wiley-Interscience, Inc., New York, 1966), p. 24.

III. RESULTS

A. General Features of Data

Twenty-seven data runs were made. The first four (covering the range 20–696°C) were done at the highest peak-to-peak (p-p) source Doppler velocity; the next four, in the region of the Curie point (744–787°C), were done at a lower p-p velocity; the nineteen subsequent runs above the Curie point (816–1413°C) were done at the lowest p-p velocity because the spectrum had collapsed to a single line with the disappearance of the nuclear magnetic field. Preceding the entire set of runs, the above three p-p velocities were calibrated by running a room-temperature iron absorption spectrum at each velocity, with the aid of known values of the ground- and excited-state splittings.[12]

Figure 3 is the Mössbauer spectrum of run 2 (at 500°C) and is typical of the five runs below the Curie point.

Runs 6–8, very near the Curie point, were the only short runs made, and their effect-to-statistics ratio is considerably poorer than that for any of the others; these three runs were used solely to locate the Curie

temperature. Figure 4 contains the spectrum of run 7, right at the Curie point. The temperature fluctuation in the oven was ±2°K. The narrow single line in Fig. 4 results from Mössbauer absorption while the absorber was above the Curie point, and the broad hump is a nearly collapsed six-line magnetic hyperfine spectrum resulting from Mössbauer absorption right below the Curie point.

Figure 5 contains the spectrum from run 21 (at 1218°C) and is typical of all spectra taken above the Curie point. The very noticeable shift in the absorption peak is due to the large relativistic and isomer shifts at elevated absorber temperature.

The percent effect for all data runs ranged from about 20% at the lowest to 1% at the highest temperatures. The full widths of the spectral lines were consistently about 0.25 mm/sec, which is 1.3 times the minimum observable width, $2(C/E)\Gamma = 0.19$ mm/sec. This is typical of the best values reported in the literature.[12]

B. Measurement of f_A and Θ

The measurements of the iron absorber recoilless fraction f_A and Debye temperature Θ fall into three
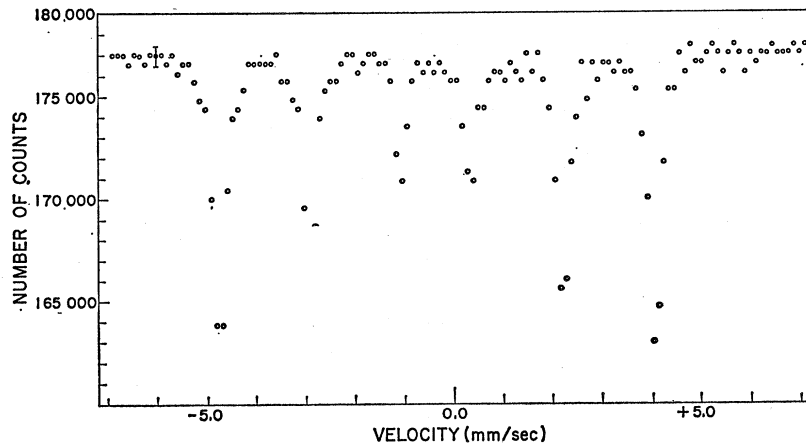

FIG. 3. Mössbauer absorption spectrum for iron at 500°C (data of run 2). The centroid of the room-temperature iron calibration spectrum is taken as zero velocity.
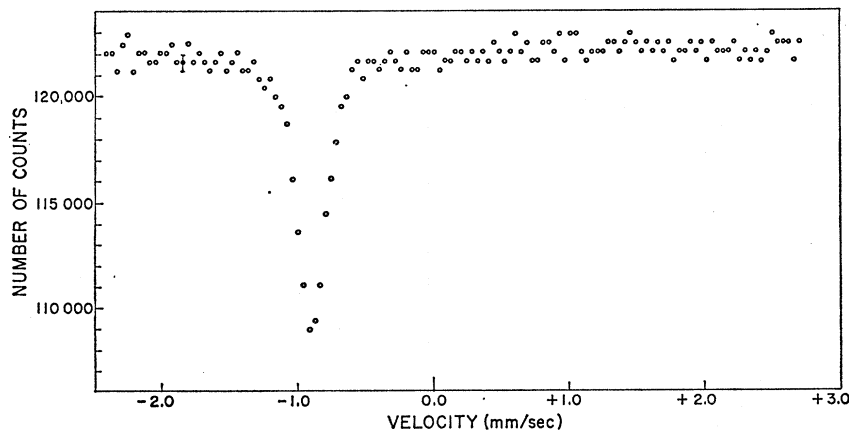

FIG. 4. Mössbauer absorption spectrum for iron at the Curie point (data of run 7). The centroid of the room-temperature iron calibration spectrum is taken as zero velocity. The superimposed broad and narrow absorption dips correspond to absorption slightly below and slightly above the Curie point, since the absorber temperature was controlled only to ±2°C.

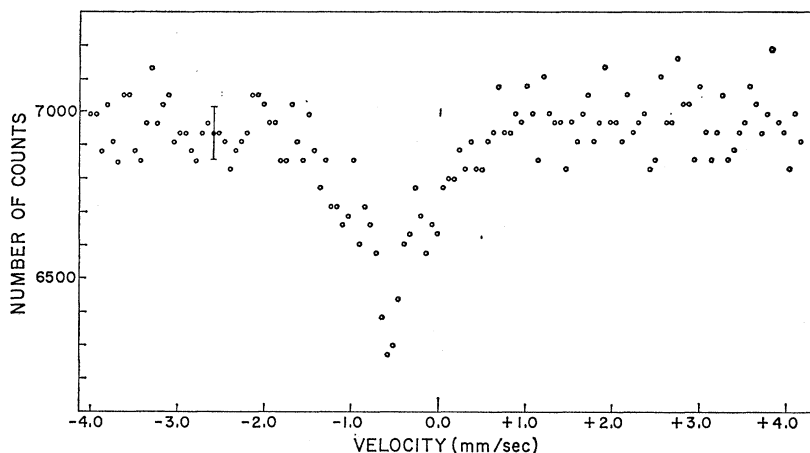[12] A. H. Muir, K. J. Ando, and H. M. Coogan (Ref. 12), p. 34.

Fig. 5. Mössbauer absorption spectrum for iron at 1218°C (data of run 21). The centroid of the room-temperature iron calibration spectrum is taken as zero velocity.

groups, corresponding to runs below the Curie point, 14 runs from the Curie point up to the temperature where the sapphire disks sandwiching the absorber cracked, and the last few runs during which the absorber slowly evaporated through the cracks.

The first five runs, from 22 to 744°C, were at absorber temperatures below the Curie point and thus yielded six-line magnetic hyperfine spectra. Table I provides the data for these. The values of f_A were calculated using the analog of Eq. (3) for multiline spectra, and Θ values were obtained from Eq. (4). Statistical errors, about ± 0.0003 for $A/\pi B$ and ± 0.005 for f_A, are not listed in this table, since they are overshadowed by the disagreement of the three values of f_A calculated for any given run: one each from the inner two spectral lines, from the middle ones, and one value from the outer ones. The discrepancies can probably be ascribed to the small number of channels per peak in the multiple-line

spectra (Fig. 3); the number of counts in a channel in this case does not really represent a point on a Lorentzian curve but rather an average over a fairly large section of the curve. Fitting a set of Lorentzians to such multiline spectra, having only $2\frac{1}{2}$ channels in the full widths of the absorption dips, could easily result in a systematic error in the analytically determined line areas. In the least-squares fitting of these data, the variance ratio was several times greater than was the case for the single-line spectra above the Curie point.

Since in this experiment the observation of the split spectra of iron below its Curie point was only a sideline, no further attention was given to the determination of f_A and Θ at low temperatures. Above the Curie point the spectrum was, of course, only a single line and the p-p Doppler velocity of the source was set lower, allowing a considerably larger number of channels per peak, as seen in Fig. 5. It may be mentioned that the most careful determination published to date of f_A in iron at room temperature was made by Hanna and Preston.[13] They obtained a value of $f_A \sigma_0 = (1.91 \pm 0.14) \times 10^{-18}/$ cm², or $f_A = 0.81 \pm 0.06$. The errors in the sub-Curie-point f_A determinations herein are not greater than the

TABLE I. f_A and Θ determinations for $T = 22$–744°C. T is the iron absorber temperature, $A/\pi B$ is the Mössbauer spectral line area divided by the product π times the base line, f_A is the absorber recoilless fraction, and Θ is the absorber Debye temperature in Tables I and II.

Run	T (°C)	Line	$A/\pi B$ (mm/sec)	f_A	Θ (°K)
1	22±1	inner	0.0078	0.88	590
		middle	0.0140	0.85	518
		outer	0.0186	0.80	437
2	500±1	inner	0.0054	0.59	449
		middle	0.0100	0.56	428
		outer	0.0125	0.50	391
3	600±1	inner	0.0046	0.49	410
		middle	0.0088	0.48	404
		outer	0.0112	0.44	382
4	696±1	inner	0.0038	0.43	397
		middle	0.0076	0.40	381
		outer	0.0099	0.38	370
5	744±1	inner	0.0036	0.41	395
		middle	0.0074	0.38	379
		outer	0.0088	0.33	354

TABLE II. f_A and Θ determinations for $T = 816$–1336°C.

Run	T (°C)	$A/\pi B$ (mm/sec)	f_A	Θ (°K)
9	816±1	0.0247±0.0002	0.291±0.004	347±2
10	878±1	0.0221±0.0003	0.250±0.004	337±2
11	908±3	0.0205±0.0003	0.227±0.004	330±2
12	928±1	0.0206±0.0003	0.228±0.004	333±2
16	930±2	0.0209±0.0003	0.233±0.005	336±3
17	931±2	0.0203±0.0004	0.224±0.005	332±2
15	933±2	0.0205±0.0003	0.227±0.004	334±1
18	934±1	0.0204±0.0003	0.226±0.005	333±3
14	937±2	0.0207±0.0002	0.230±0.003	336±1
13	950±1	0.0209±0.0004	0.233±0.006	339±3
19	1019±3	0.0182±0.0003	0.195±0.004	329±2
20	1115±1	0.0156±0.0003	0.161±0.003	322±2
21	1218±1	0.0128±0.0003	0.128±0.004	315±2
22	1336±4	0.0096±0.0003	0.092±0.003	304±1

[13] S. S. Hanna and R. S. Preston, Phys. Rev. 139A, 722 (1965).

errors of Hanna and Preston, and the room-temperature values in this experiment agree reasonably well with theirs.

The next three data runs, 6–8, were just short runs to locate the Curie point and no line-area determinations were attempted for these. Fourteen runs (9–22), at 816–1336°C, were carried out above the Curie point before the sapphire disks protecting the absorber cracked. These are listed in Table II in order of increasing temperature. The recoilless fraction f_A was calculated from Eq. (3), and Θ was obtained from Eq. (4).

Figure 6 is a plot of f_A versus absorber temperature from 22 to 1336°C and Fig. 7 is a plot of Θ for the same temperature range. From analytic fits to the data points between phase transitions, the values of the discontinuities in f_A and Θ at the α-γ transition are

$$(\delta f_A)_{\alpha\gamma} = +0.030 \pm 0.008,$$

$$(\delta\Theta)_{\alpha\gamma} = +(8\pm3)°\text{K}.$$

The Debye temperature of a solid may be written

$$\Theta = (h/k)\nu_s(3\pi N/V)^{1/3}, \tag{5}$$

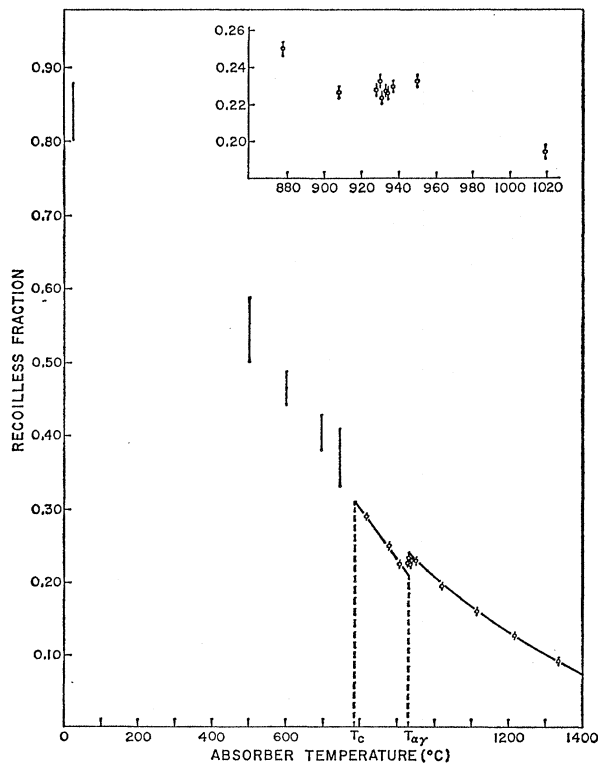where N is the number of atoms in the solid, V is its volume, and the velocity of sound is given in the

Fɪɢ. 6. Recoilless fraction f_A of Fe⁵⁷ in metallic iron from 22 to 1336°C. T_c is the Curie temperature and $T_{\alpha\gamma}$ locates the α-γ transition. The large error bars on the points below T_c are due to the difficulty of accurately determining f_A from multiline spectra with only a few analyzer channels per peak. The insert shows the details of the data near $T_{\alpha\gamma}$.
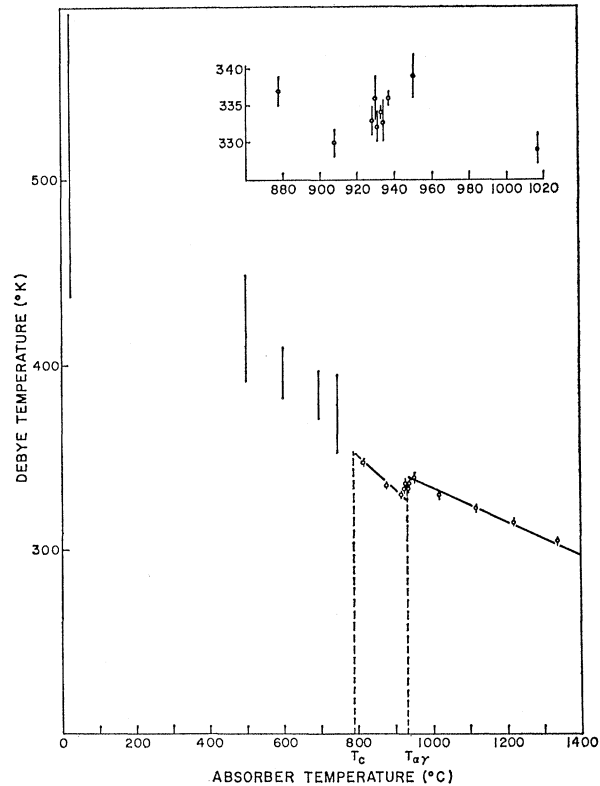
Fɪɢ. 7. Debye temperature of metallic iron from 22 to 1336°C, derived from recoilless fraction data in Fig. 6. T_c is the Curie temperature and $T_{\alpha\gamma}$ is the α-γ transition temperature. The insert shows the details of the data near $T_{\alpha\gamma}$.

simplest approximation by

$$\nu_s = (CV/N)^{1/2}, \tag{6}$$

where C is the adiabatic bulk elastic constant of the solid. Equations (5) and (6) yield

$$\Theta = C^{1/2}(V/N)^{1/6}. \tag{7}$$

With this equation, using Köster's measurements[14] of Young's modulus for C and the data of Basinski et al.[15] on volume expansion for iron, we obtain the estimate

$$(\delta\Theta)_{\alpha\gamma} = +19°\text{K},$$

which agrees reasonably well with the Mössbauer value, inasmuch as Young's modulus is only a rough estimate of the elastic constant C called for in Eq. (7).

Following run 22 at 1336°C, the sapphire disks protecting the absorber cracked and direct measurements of f_A and Θ could not be made for runs 23–27, since the absorber slowly evaporated through the cracks and the amount of iron left in the foil was not known. Figure 8 is a graph of the Mössbauer spectral line areas for the runs above 1000°C. The energy shift data in Sec. III C (see Fig. 9) indicate that the runs at temperatures

[14] W. Köster, Z. Metallkunde **39**, 1 (1948).

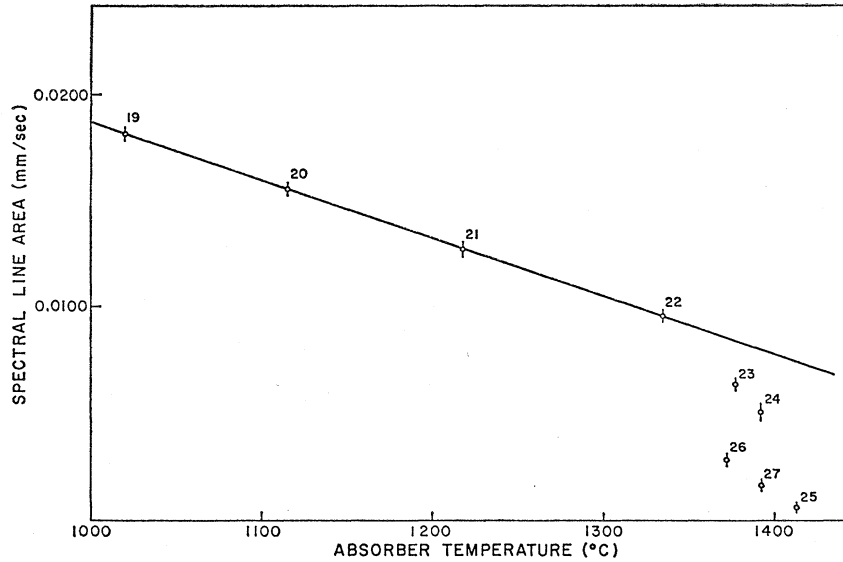[15] Z. S. Basinski, H. Hume-Rothery, and A. L. Sutton, Proc. Roy. Soc. (London) **A229**, 459 (1955).

Fig. 8. Normalized Mössbauer spectral line area $A/\pi B$ in iron for absorber temperature $T=1000$–$1413°C$. The measured areas for the last five runs (23–27) are too low because the absorber was evaporating during these runs. Run numbers are shown to indicate the order in which the points were determined.

1393°C and below are definitely below the γ-δ point. Thus the values of line area, recoilless fraction, and Debye temperature for runs 23, 24, 26, and 27 can be obtained simply by reading the numbers off Figs. 8, 6,
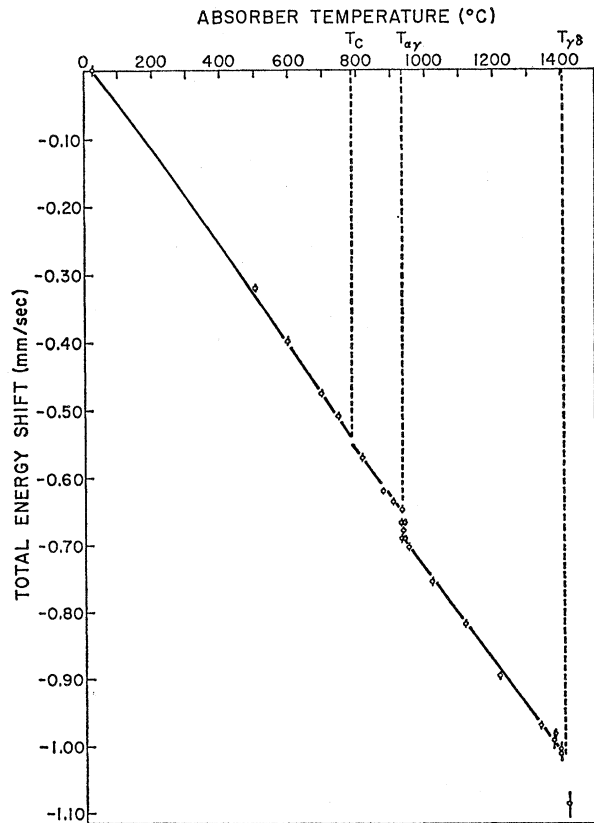

Fig. 9. Total observed energy shift of Fe^{57} in a metallic iron absorber from 22 to 1413°C. The shift is taken as zero at 22°C. T_c is the Curie temperature and $T_{\alpha\gamma}$ and $T_{\gamma\delta}$ are the α-γ and γ-δ phase-transition temperatures.

and 7 (extrapolated to 1393°C). Then the actually measured and the extrapolated line-area values may be used to calculate the correction factor for getting the true line area from the measured value, as shown in Table III. The point of this is that the value of the line-area correction factor for run 25 (at 1413°C) must lie between the correction factor for runs 24 and 26. From Table III it is seen that the line-area correction for run 25 may safely be taken as 2.3 ± 0.7; applying this to the measured value of $A/\pi B=0.0006\pm0.0002$ mm/sec yields the following corrected values for run 25 (1413°C):

$$A/\pi B = 0.0014\pm0.0006 \text{ mm/sec},$$

$$f_A = 0.012\pm0.006,$$

$$\Theta = (226\pm14)°\text{K}.$$

Comparing these to the extrapolated γ-phase values for 1413°C, also listed in Table III, we obtain the following estimates:

$$(\delta f_A)_{\gamma\delta} = -(0.06\pm0.-1), \quad (\delta\Theta)_{\gamma\delta} = -(70\pm15)°\text{K}.$$

The Mössbauer value of $(\delta\Theta)_{\gamma\delta}$ cannot be independently checked because there are no data on the variation of the elastic constant of iron in the region of the γ-δ transition.

C. Energy-Shift Measurements

The position of the centroid of the Mössbauer absorption spectrum was determined for all of the data runs. The shift of the 22°C spectrum was taken as zero, and the energy-shift values at all other temperatures are measured relative to the position of the centroid of the 22°C spectrum. Since the temperature of the source is held fixed, the energy shift $\Delta(E_A-E_S)$ in the centroid of the Mössbauer absorption spectrum is simply equal to the change ΔE_A in the resonant absorption energy E_A of the iron absorber, which varied because of the

TABLE III. Extrapolation of γ-phase values of line area $A/\pi B$, recoilless fraction f_A, and Debye temperature Θ.[a]

Run	T (°C)	Measured $A/\pi B$ (mm/sec)	γ-phase extrapolated $A/\pi B$ (mm/sec)	$A/\pi B$ correction factor	γ-phase extrapolated f_A	γ-phase extrapolated Θ (°K)
23	1377	0.0064	0.0084	1.3	0.079	300
24	1393	0.0051	0.0079	1.6	0.074	298
26	1372	0.0028	0.0085	3.0	0.080	300
27	1393	0.0016	0.0079	4.9	0.074	298
⋯	1413	⋯	0.0074	⋯	0.069	296

[a] These numbers are read off the graphs in Figs. 8, 6, and 7, and include the area correction factors for the four runs right under the γ-δ transition; the area correction factor is the extrapolated area value divided by the measured area value. The measured line-area values for these runs were incorrect because of absorber evaporation.

temperature dependence of the isomer shift and the relativistic shift in the absorber. Experimental values of ΔE_A are given in velocity units in Table IV.

A plot of these data is given in Fig. 9. As mentioned, the data of the short runs 6–8 were used only to locate the Curie point; the statistical errors in these runs are very large, so these data are omitted from the energy-shift table and plot. It was noted in the previous section that because the sapphire disks cracked after the 1336°C run, direct measurements of f_A and Θ could not be made above this temperature, since the iron slowly evaporated through the cracks. This did not prevent a measurement of the spectral line *position* for the last five runs, however; and it was possible to measure the energy shift ΔE_A up to a temperature (1413°C) past the γ-δ phase transition.

The three discontinuities in the total shift (Fig. 9) locate the Curie point, the α-γ phase transition, and the γ-δ phase transition. It is noted from Figs. 6 and 9 that the discontinuities in the recoilless fraction data and the energy-shift data agree on the location of the α-γ transition (at about 930°C). As noted herein, the energy-shift data clearly indicate the location of the γ-δ transition point, and this information was useful in determining estimates of f_A and Θ values for the last five runs, where the absorber was evaporating.

The discontinuity at the Curie point was first seen by Preston et al.[1,16] and is discussed by Alexander and Treves.[17] The large discontinuities in the energy shift at the two phase transitions are due to changes in the isomer shift with the changes in crystal structure. The discontinuity at the α-γ transition was first seen by Preston et al.[1] Because crystal structure changes are accompanied by a discontinuous volume change, we would expect to see a discontinuous change in the energy shift given by

$$\frac{\delta E_A/E_A}{\delta V/V} = \left(\frac{\partial \ln E_A}{\partial \ln V}\right)_T^{\text{isom}} + \left(\frac{\partial \ln E_A}{\partial \ln V}\right)_T^{\text{rel}}. \quad (8)$$

If we assume that only the $4s$ atomic electron wave functions are changed on volume expansion, and that

[16] R. S. Preston, Phys. Rev. Letters **19**, 75 (1967).
[17] S. Alexander and D. Treves, Phys. Letters **20**, 134 (1966).

the $4s$ electron density scales with volume, we obtain[18–20]

$$(\partial \ln E_A/\partial \ln V)_T^{\text{isom}}$$
$$= (4.3\pm0.5)\times10^{-12}(1-\Delta V/V_0), \quad (9)$$

where V_0 is room-temperature volume and ΔV is the change relative to V_0. Also,[18]

$$\left(\frac{\partial \ln E_A}{\partial \ln V}\right)_T^{\text{rel}} = -\frac{3k\Theta}{2m_A c^2} - \frac{\Theta}{T}\left(\frac{\partial \ln\Theta}{\partial \ln V}\right)_T \quad (10)$$

gives the second term in Eq. (8). Since the α-γ and γ-δ transitions take place at temperatures much higher than

TABLE IV. Total observed energy shift of Fe[57] in iron from the Mössbauer absorption spectra for $T=22–1413$°C. The values $(C/E_A)\Delta E_A$ are in velocity units; the shift is taken as zero at 22°C.

Run	T (°C)	$(C/E_A)\Delta E_A$ (mm/sec)
1	22±1	0.000
2	500±1	−0.319±0.003
3	600±1	−0.397±0.004
4	696±1	−0.477±0.004
5	744±1	−0.509±0.003
9	816±1	−0.570±0.002
10	878±1	−0.621±0.003
11	908±3	−0.636±0.003
12	928±1	−0.648±0.003
16	930±2	−0.668±0.003
17	931±2	−0.667±0.003
15	933±2	−0.690±0.003
18	934±1	−0.681±0.003
14	937±2	−0.693±0.003
13	950±1	−0.706±0.003
19	1019±3	−0.755±0.003
20	1115±1	−0.818±0.003
21	1218±1	−0.893±0.004
22	1336±4	−0.969±0.005
26	1372±3	−0.989±0.010
23	1377±4	−0.982±0.006
24	1393±2	−1.013±0.010
27	1393±4	−1.008±0.004
25	1413±2	−1.087±0.022

[18] R. V. Pound, G. B. Benedek, and R. Drever, Phys. Rev. Letters **7**, 405 (1961).
[19] D. N. Pipkorn, C. K. Edge, P. Debrunner, G. DePasquali, H. G. Drickamer, and H. Frauenfelder, Phys. Rev. **135A**, 1604 (1964).
[20] L. R. Walker, G. K. Wertheim, and V. Jaccarino, Phys. Rev. Letters **6**, 98 (1961).

the Debye temperature, we can show from Eqs. (9) and (10) that the relativistic shift term in Eq. (8) is at least two orders of magnitude smaller than the isomer-shift term at these two transitions. So we have for the expected discontinuity of the shift (in velocity units)

$$(C/E_A)(\delta E_A) = C(\partial \ln E_A/\partial \ln V)_T{}^{\text{isom}}(\delta V/V). \quad (11)$$

Straight-line-segment fits were made to the data in Fig. 9 for temperatures 816°C and above. At the α-γ transition, $(\delta E_A)_{\alpha\gamma}$ was evaluated by subtracting the values for the α-phase fit at 930°C from the value of the γ-phase fit at 930°C, giving

$$(C/E_A)(\delta E_A)_{\alpha\gamma} = -(0.041\pm0.004) \text{ mm/sec}.$$

But if $(\partial \ln E_A/\partial \ln V)_T{}^{\text{isom}}$ is obtained from Eq. (9) and $\delta V/V$ is taken from the volume expansion data of Basinski *et al.*,[15] we obtain

$$C\left(\frac{\partial \ln E_A}{\partial \ln V}\right)_T{}^{\text{isom}} \frac{(\delta V)_{\alpha\gamma}}{V} = -(0.013\pm0.002) \text{ mm/sec},$$

which leaves a residual value of $-(0.028\pm0.005)$ mm/sec to be accounted for in the isomer-shift discontinuity at $T_{\alpha\gamma}$.

Similarly, for the γ-δ transition, $(C/E_A)(\delta E_A)_{\gamma\delta} = -(0.07\pm0.02)$ mm/sec but

$$C\left(\frac{\partial \ln E_A}{\partial \ln V}\right)\frac{(\delta V)_{\gamma\delta}}{V} = +(0.007\pm0.001) \text{ mm/sec},$$

which leaves a jump of $-(0.08\pm0.02)$ mm/sec unexplained in $(C/E_A)(\delta E_A)_{\gamma\delta}$, four times as large and of the same sign as the unexplained part of $(C/E_A)(\delta E_A)_{\alpha\gamma}$.

It is worth noting that the discontinuity in the energy shift is not only too large but also in the wrong direction to be explained by Eq. (9) at $T_{\gamma\delta}$. At the α-hcp phase transition in iron under high pressures, Pipkorn *et al.*[19] observe a similar discontinuity in the isomer shift which is several times too large to be explained by Eq. (9). They say that the large shift must be related to a difference in the band structure of the two phases and cite several mechanisms without attempting to make any calculations.

It has not been possible in the present experiment to construct a quantitative theoretical explanation of the large size of these discontinuities in the isomer shift in iron at phase changes, nor were any attempts to do this found in the literature.

Semiclassical Theory of a High-Intensity Laser*

STIG STENHOLM† AND WILLIS E. LAMB, JR.

Department of Physics, Yale University, New Haven, Connecticut 06520

(Received 30 September 1968)

This paper extends the calculations of the semiclassical Lamb theory of a Doppler-broadened gas laser (optical maser) to arbitrary intensities for the case of single-mode operation. The coupled equations of the classical electromagnetic field and an ensemble of two-level atoms are set up, and a solution is obtained in the form of a continued fraction. This is used to compute intensity-detuning curves and atomic population inversion densities as functions of both the velocity and the position in the laser. When the laser is tuned to resonance, the velocity dependence of the inversion density shows a previously unknown fine structure consisting of a "bump" in the bottom of the hole. The calculations are compared to results obtained from a perturbation expansion in powers of the field and exact results known for atoms with zero velocity. The response of the laser output to a slow modulation and the buildup of oscillations are also discussed.

1. INTRODUCTION

THE semiclassical theory of gas lasers given by Lamb[1,2] is capable of explaining, at least qualitatively, most observed features of the operation. These include the detuning dip[3] and mode competition effects.[4] Extensions of the theory to the cases of Zeeman lasers[5] and ring lasers[6] have been given and pressure effects on the laser performance have been considered.[7] Only laser characteristics which intrinsically depend on

[1] W. E. Lamb, Jr., Phys. Rev. **134**, A1429 (1964).

[2] W. E. Lamb, Jr., in *Quantum Optics and Electronics*, edited by C. DeWitt, A. Blandin, and C. Cohen-Tannoudji (Gordon and Breach, Science Publishers, Inc., New York, 1965).

[3] R. A. McFarlane, W. R. Bennett, Jr., and W. E. Lamb, Jr., Appl. Phys. Letters **2**, 189 (1963); A. Szöke and A. Javan, Phys. Rev. Letters **10**, 521 (1963); Phys. Rev. **145**, 137 (1966).

[4] R. L. Fork and M. A. Pollack, Phys. Rev. **139**, A1408 (1965); J. Haisma and G. Bouwhuis, Phys. Rev. Letters **12**, 287 (1964); W. J. Witteman and J. Haisma, *ibid.* **12**, 617 (1964); W. J. Witteman, Phys. Rev. **143**, 316 (1966).

[5] R. L. Fork and M. Sargent III, Phys. Rev. **139**, A617 (1965); M. Sargent III, W. E. Lamb, Jr., and R. L. Fork, *ibid.* **164**, 436 (1967); **164**, 450 (1967); W. J. Tomlinson, M. A. Pollack, and R. L. Fork, Appl. Phys. Letters **11**, 150 (1967); W. J. Tomlinson and R. L. Fork, Phys. Rev. **164**, 466 (1967).

[6] B. L. Gyorffy and W. E. Lamb, Jr. (to be published).

[7] B. L. Gyorffy, M. Borenstein, and W. E. Lamb, Jr., Phys. Rev. **169**, 340 (1968).